Single-Stage Grid-Connected Forward Microinverter with Boundary Mode Control

D. Meneses, O. García, P. Alou, J. A. Oliver, R. Prieto, J. A. Cobos
Universidad Politécnica de Madrid
Centro de Electrónica Industrial
Madrid, Spain
cei@upm.es

***Abstract*— This paper presents a microinverter to be integrated into a solar module. The proposed solution combines a forward converter and a constant off-time boundary mode control, providing MPPT capability and unity power factor in a single-stage converter. The transformer structure of the power stage remains as in the classical DC-DC forward converter. Transformer primary windings are utilized for power transfer or demagnetization depending on the grid semi-cycle. Furthermore, bidirectional switches are used on the secondary side allowing direct connection of the inverter to the grid. Design considerations for the proposed solution are provided, regarding the inductance value, transformer turns ratio and frequency variation during a line semi-cycle. The decoupling of the twice the line frequency power pulsation is also discussed, as well as the maximum power point tracking (MPPT) capability. Simulation and experimental results for a 100W prototype are enclosed.**

I. INTRODUCTION

The interest in exploring renewable energies has grown in the last years. Photovoltaic (PV) sources are predicted to have the highest increase (30%) in the next decade and to be the biggest contributor on the electricity generation in 2040, among the renewable energy sources [1]. Within PV systems, power inverters are required to inject the PV energy into the AC grid. In [2] a historical evolution of the PV inverters is presented. Nowadays, the AC-module (PV panel with an integrated inverter) technology is becoming more and more popular [3-5] instead of centralized, string and multi-string inverter technologies. This is due to its modularity and the possibility of single panel maximum power point tracking (MPPT), as well as safe and simple installation ("plug and play") [2,6].

Regarding the single-phase grid-connected inverters utilized in the AC-module [2,4,6,7], some similarities can be found with the power factor correction (PFC) application. In [8], an AC-module with a control complying with IEC 61000-3-2 is considered a kind of PFC injecting current instead of consuming it. In [9] a transformerless inverter based on a PFC converter is proposed and in [10] a power decoupling method, to handle the difference between the instantaneous output power and the constant input power, is implemented to reduce the input capacitance.

The electrical specifications in AC-module applications are: low input voltage range (up to 50V), high output voltage (230V in Europe or 110V in USA) and nominal power up to 500W. Due to that, simple, single-stage and isolated topologies, as flyback inverter [15], are preferred.

In this paper a simple and low-cost single-stage high-frequency link inverter for a PV module is presented in section II. This low power microinverter is based on a forward converter applying the boundary conduction mode control commonly used in PFC applications [11]. The proposed solution provides unity power factor and integrates the MPPT function capability. Converter operation for both positive and negative grid voltage is presented in section III, while design considerations are provided in section IV. Finally, simulation and experimental results for 110V, 60Hz main are presented in sections V and VI respectively.

II. PROPOSED SOLUTION

An AC-module integrates a PV panel and an inverter [5], also known as microinverter or module integrated converter (MIC) [4]. Microinverter is a low-cost, low-weight, as well as a reliable converter and for these reasons, a simple topological solution with few components and high-frequency isolation is preferred. Furthermore, the converter integrates the MPPT function [12] and PFC.

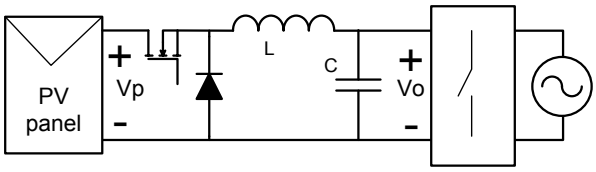

Figure 1. Buck converter connected between a PV panel and the grid.

In Fig. 1 a buck converter is connected between the solar panel and the grid, thus working as a current source. Fig. 2 illustrates the inductor current waveform in the boundary between continuous and discontinuous conduction mode during a grid half-period and a switching period respectively. The switch is turned on as the inductor current reaches zero

and turned off when it reaches a sinusoidal envelope. Thus the averaged current is sinusoidal, as in the boost converter utilized in PFC applications.

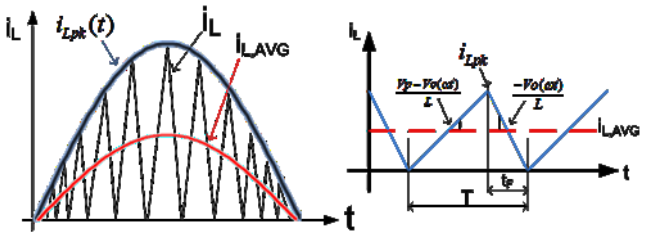

Figure 2. Buck inductor current within a grid half-period and within a switching period.

The average value of the inductor current can be easily obtained from the inductor current waveform within a switching period (Fig. 2). The resulted expression is presented in (1).

$$i_{L,AVG} = \frac{1}{2}\cdot i_{Lpk} = \frac{1}{2}\cdot\frac{Vo(\omega t)}{L}\cdot t_F = K\cdot Vo(\omega t), \text{if } t_F = const. \quad (1)$$

Therefore, as the average value of the inductor current is the output current of the buck converter, the current injected to the grid is sinusoidal (proportional to the grid voltage) if the off-time is kept constant.

The utilization of a buck converter requires a solar panel voltage higher than the grid peak voltage, which in case of European 230V grid means more than 300V. Therefore, the utilization of a transformer is necessary in order to use most of the commercial solar modules, having the output voltages between 20V and 50V.

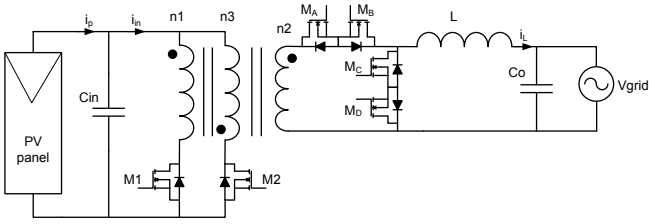

Figure 3. Proposed forward boundary mode control microinverter.

Several isolated buck-derived topologies can be used. However, due to the low power range of the commercial PV modules, simple topologies as forward converter are preferred. The proposed forward microinverter is shown in Fig. 3.

III. CONVERTER OPERATION

The forward converter is a well-known topology [13] within the DC-DC converters. However, since the goal is to connect the AC-module directly to the grid, in order to keep the transformer structure as in DC-DC applications, bidirectional switches are used in the secondary side.

Secondary side transistors are line frequency switched: MA and MD for positive line voltage, and MB and MC for

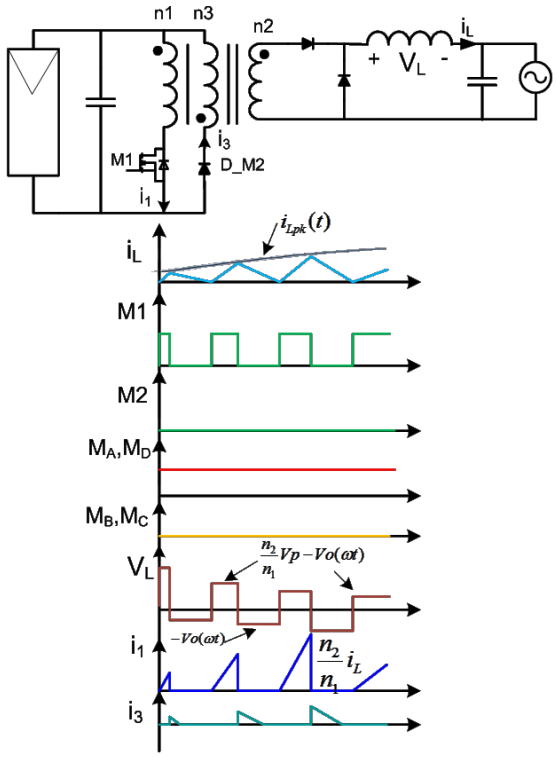

Figure 4. Equivalent subcircuit and main waveforms of the proposed microinverter for positive grid voltage.

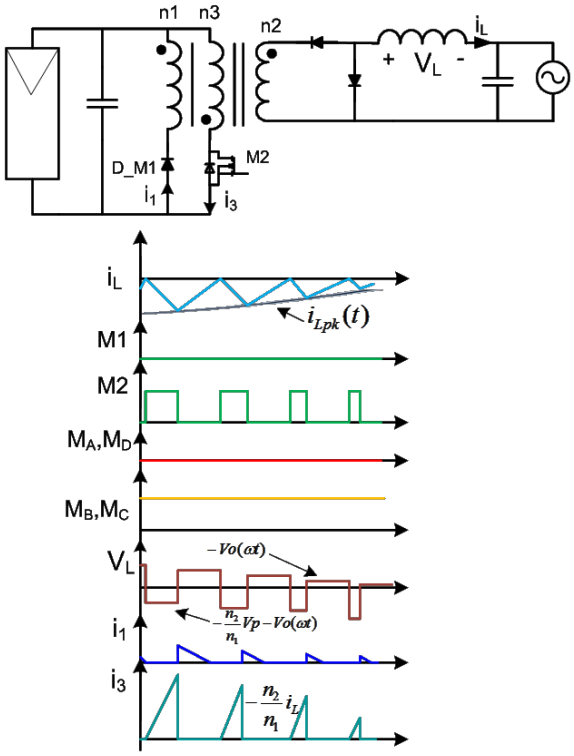

Figure 5. Equivalent subcircuit and main waveforms of the proposed microinverter for negative grid voltage.

the negative semi-cycle. Regarding the primary side, M1 and M2 are switched applying the above mentioned control method in the correspondence line semi-cycle: M1 during the positive semi-period and M2 during the negative one. Transformer demagnetization within the proposed topology is done by means of the primary winding that is not utilized for the power transfer, as in a classical forward converter.

Thus the converter behaves differently depending on the line voltage polarity. Fig. 4 and Fig. 5 show the switches control signal and the main waveforms for both line voltage semi-cycles. Note that the line switched transistors have been removed in the equivalent circuits.

IV. DESIGN CONSIDERATIONS

A. *Variable frequency operation:*

The proposed control method assumes that t_F remains constant during the inverter operation, as it was introduced previously. Therefore, this control method implies variable frequency operation. Fig. 6 shows the frequency variation during a half line period. The relation between the off-time (t_F) and the period (T) can be derived based on the inductor current waveform presented in Fig. 2, introducing the turn ratio of the forward transformer. The minimum frequency is obtained at the peak value of the line voltage while the maximum frequency is limited for the off-time when the line voltage crosses zero.

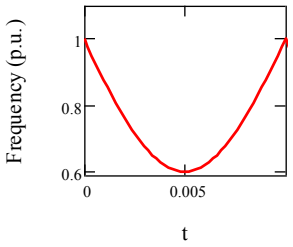

$$f_{sw}(t) = \left(1 - \frac{|Vo(\omega t)|}{\frac{n_2}{n_1} \cdot Vp}\right) \cdot \frac{1}{t_F}$$

Figure 6. Frequency variation in a grid half-period.

B. *Inductance value:*

As introduced in (1), if the off-time is kept constant, the output current is proportional to the output voltage. Utilizing this result in the calculation of the delivered output power, the relation between the output power and the inductance value is achieved (2).

$$Po = \frac{1}{2} \cdot Vo_{pk} \cdot Io_{pk} = \frac{1}{2 \cdot L} \cdot Vo_{RMS}{}^2 \cdot t_F \tag{2}$$

C. *Input capacitor (power decoupling):*

Based on the fact that the current provided by the solar panel is pure DC (i_p on Fig. 7) and the current demanded by the inverter ($i_{in,AVG}$) follows a square sinusoidal waveform, power decoupling is needed in the converter. Usually, this power decoupling is done by means of a capacitor either at the input of the converter or at a DC link, which requires two-stage converters or auxiliary circuits [10]. The aim to use a DC link is to keep the capacitance as low as possible in order to utilized ceramic capacitors.

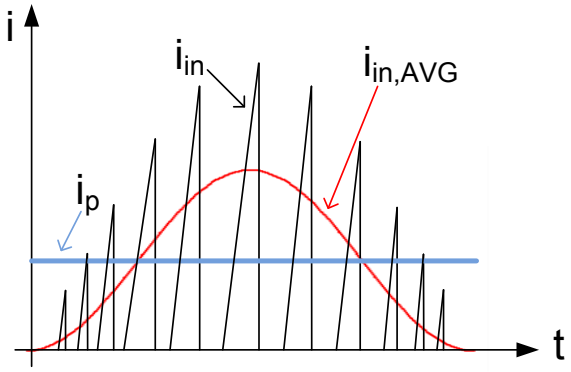

Figure 7. Instantaneous (i_{in}) and average ($i_{in,AVG}$) input current and solar panel current (i_p) during a line half-period.

In the proposed solution the decoupling function is performed by electrolytic capacitors in parallel with the solar panel. Equation (3) [2] provides the capacitance necessary for a solar panel output voltage and power, and for a given voltage ripple ($\hat{u}_C$). Since the capacitor voltage is the panel voltage, the voltage ripple has a significant impact on the photovoltaic module, resulting in a lower power generation [2].

$$Cin = \frac{P_{PV}}{2 \cdot \omega_{grid} \cdot U_C \cdot \hat{u}_C} \tag{3}$$

D. *Forward transformer*

As it shown in Fig. 3, the transformer structure of this forward inverter is the same than in a classical DC-DC forward converter. Both primary windings are utilized alternately for power transfer and demagnetization, depending on the line voltage semi-cycle. Therefore, the turns ratio between the two primary windings is required to be the same, and the maximum applicable duty cycle in the primary transistors is limited to 0.5 (4), in order to guarantee the transformer demagnetization [13].

$$n_1 = n_3 \Rightarrow d_{\max} = 0.5 \tag{4}$$

The secondary to primary turns ratio (5) has to be designed to achieve the line peak voltage for the minimum input voltage (Vp_{min}), taking into account the duty cycle limitation.

$$\left(\frac{n_2}{n_1}\right)_{\min} = \frac{Vo_{pk}}{d_{\max} \cdot Vp_{\min}} \tag{5}$$

E. *MPPT function*

The power available in the system is provided by the solar panel. An outer control loop to track the maximum

power point of the PV panel can be implemented either in a digital device [16] or analog implementation [17] as in other two-stage or single-stage inverters.

In the proposed control, the output current peak in (2) is related with the inductor peak current envelope as is shown in Fig. 2. Therefore, the proposed control method allows the MPPT function by means of the modulation of the inductor current envelope with the control signal generated by above mentioned outer loop.

V. SIMULATION RESULTS

A simulation model of the proposed solution has been developed. Fig. 8 shows the inductor and the output current during a half semi-cycle for both positive and negative 110V, 60Hz line voltage, with an input voltage of 30V.

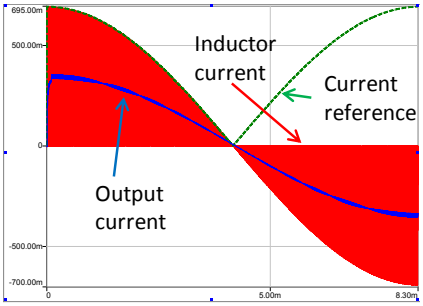

Figure 8. Output and inductor current simulation results.

Fig. 9 presents the drain to source voltage of the transistor M1 (Fig. 3) as well as the inductor current and the current through the winding n_3. In Fig. 9.a the line voltage is positive and the winding n3 is utilized to demagnetize the transformer. However, as illustrated in Fig. 7.b the line voltage is negative and the power transfer occurs through the same winding.

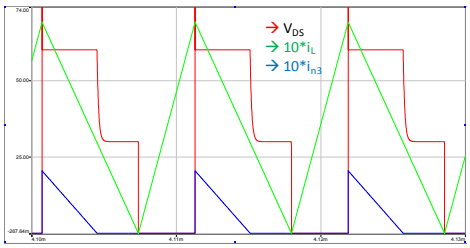

a

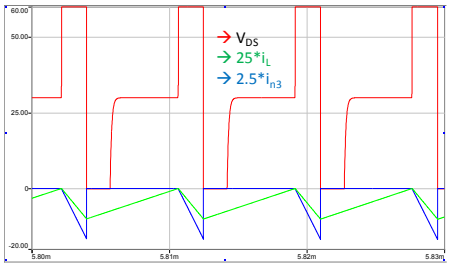

b

Figure 9. Simulated drain to source voltage, transformer current and inductor current for positive (a) and negative (b) line voltage.

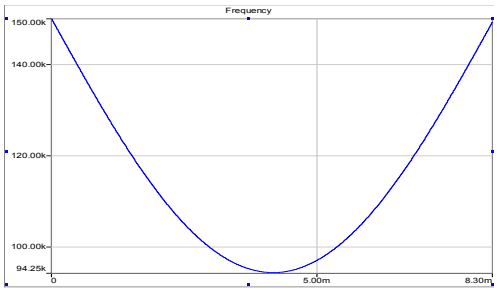

Figure 10. Simulated frequency variation during one semi-cycle.

Results presented in Fig. 9 have a time range of 30µs, thus the operation frequency is different in Fig. 9.a than in Fig. 9.b, as expected. Fig. 10 shows the frequency variation during a line voltage semi-cycle, obtained from the simulation model.

VI. EXPERIMENTAL RESULTS

A 30V input voltage and 100W prototype (Fig. 11), with 230V output voltage, for the proposed microinverter is built to validate the proposed solution.

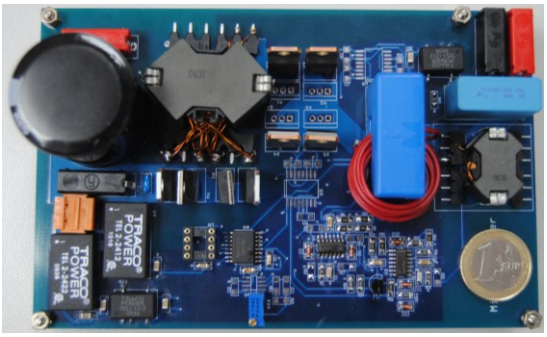

Figure 11. Forward microinverter prototype.

The control stage has been implemented utilizing a boundary mode PFC commercial controller: UCC38050. Fig. 12 shows a block diagram of the implemented converter, with the main waveforms in the control stage. Both the inductor current and the output voltage are measured with Hall Effect sensors. As in PFC applications, the voltage and the current are measured after the rectifier, the controller operates only with positive voltages. Thus, the output voltage and inductor current measurements require to be rectified. Furthermore, the inductor voltage changes the polarity with the line voltage. In order to ensure the proper zero current detection (ZCD) using the inductor voltage [14], a multiplier is used.

The MPPT function described in the design considerations section can be implemented with the used controller. The MPPT algorithm would change the inductor current envelope by placing a DC signal in the controller pin that is used to implement the voltage loop in PFC applications.

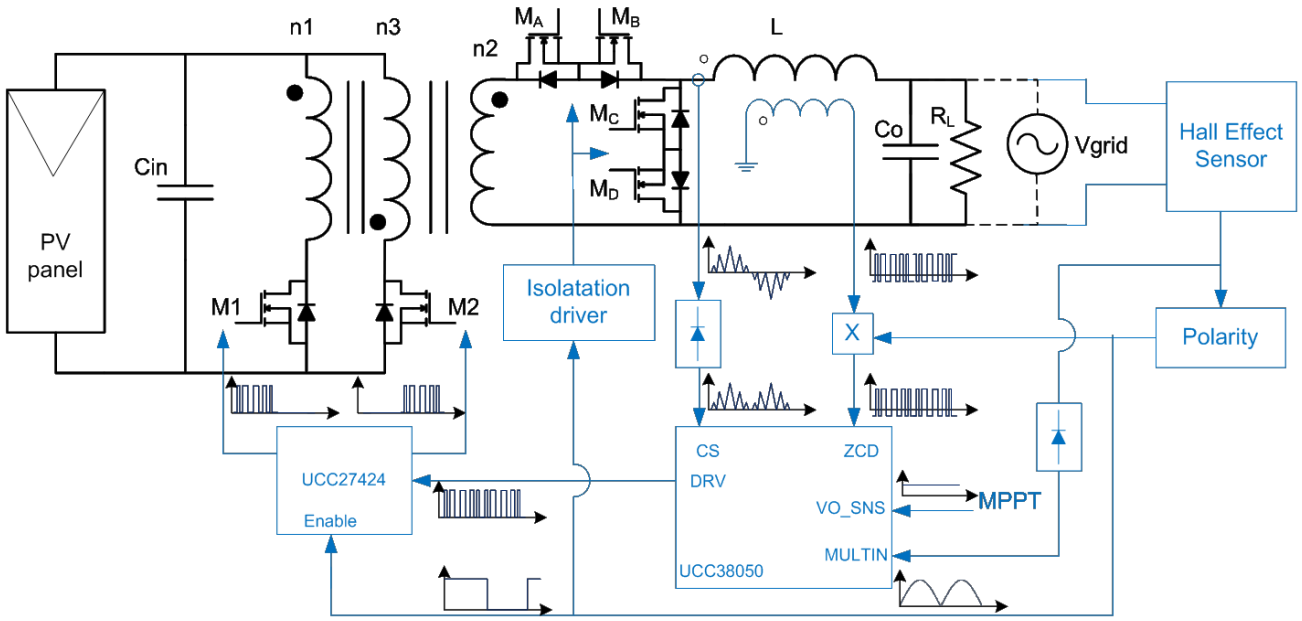

Figure 12. Block diagram of the implemented circuit (power and control stages) with the main waveforms in the control stage.

Finally, isolated drivers are used to drive the secondary side floating MOSFET. Regarding the primary side transistors, a dual driver with enabled outputs (UCC27424) is utilized.

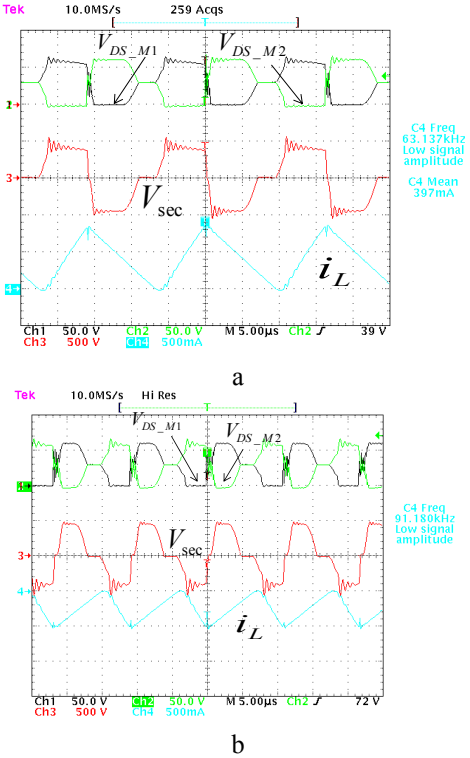

Figure 13. Waveforms of the proposed forward microinverter for positive (a) and negative (b) output DC voltage.

Fig. 13.a and Fig. 13.b show the drain to source voltage of the primary side transistors (V_{DS_M1}, V_{DS_M2}), the transformer secondary side voltage (Vsec) and the inductor current (i_L) for positive and negative output DC voltage respectively.

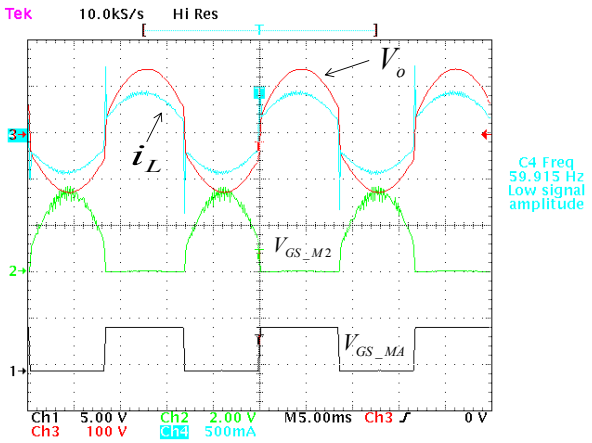

Figure 14. Control signals and output waveforms at 60Hz operation.

Fig. 14 shows the achieved AC results utilizing a resistor as a load and replacing the grid by an external AC 110V and 60Hz power source to generate the current reference, as shown in Fig. 12. As the results are achieved for an output voltage of 110V, in order to avoid inductor saturation, the obtained output power has been 50W, with an efficiency of 81% for the test shown in Fig. 14. The challenging physical implementation of the transformer hindered to achieve the expected results regarding the desired output voltage level. Furthermore, zero cross behavior has to be analyzed and optimized.

VII. CONCLUSIONS

In this paper a simple and low-cost forward microinverter based on the boundary mode control, with constant off-time, is presented. The proposed one-stage converter integrates MPPT function capability and is directly connected to the AC grid, injecting unity power factor current. Furthermore, the transformer configuration remains as in the classical forward converter allowing power transfer and demagnetization for both positive and negative line voltage. Design considerations regarding the turns ratio, frequency variation, output power and input capacitor are presented and validated by simulation. The concept of the proposed solution, as well as the use of a PFC commercial controller has been validated by the experimental results. Nevertheless, several issues such as transformer design and zero cross behavior need to be further analyzed and optimized.

REFERENCES

[1] http://www.erec.org/media/publications/2040-scenario.html

[2] Kjaer, S.B.; Pedersen, J.K.; Blaabjerg, F.; "A review of single-phase grid-connected inverters for photovoltaic modules," Industry Applications, IEEE Transactions on , vol.41, no.5, pp. 1292- 1306, Sept.-Oct. 2005.

[3] Calais, M.; Myrzik, J.; Spooner, T.; Agelidis, V.G.; "Inverters for single-phase grid connected photovoltaic systems-an overview," *Power Electronics Specialists Conference, 2002. pesc 02. 2002 IEEE 33rd Annual* , vol.4, no., pp. 1995- 2000, 2002

[4] Quan Li; Wolfs, P.; "A Review of the Single Phase Photovoltaic Module Integrated Converter Topologies With Three Different DC Link Configurations," *Power Electronics, IEEE Transactions on* , vol.23, no.3, pp.1320-1333, May 2008

[5] Wills, R.H.; Krauthamer, S.; Bulawka, A.; Posbic, J.P.; "The AC photovoltaic module concept," Energy Conversion Engineering Conference, 1997. IECEC-97., Proceedings of the 32nd Intersociety, vol.3, no., pp.1562-1563 vol.3, 27 Jul-1 Aug 1997

[6] Nasser Kutkut, Haibing Hu, University of Central Florida, "Photovoltaic Microinverters: Topologies, Control Aspects, Reliability Issues, and Applicable Standards"; ECCE 2010, tutorial.

[7] Jih-Sheng Lai; "Power conditioning circuit topologies," *Industrial Electronics Magazine, IEEE* , vol.3, no.2, pp.24-34, June 2009

[8] Fernandez, A.; Sebastian, J.; Hernando, M.M.; Arias, M.; Perez, G.; , "Single Stage Inverter for a Direct AC Connection of a Photovoltaic Cell Module," *Power Electronics Specialists Conference, 2006. PESC '06. 37th IEEE* , vol., no., pp.1-6, 18-22 June 2006.

[9] Araujo, S. V.; Zacharias, P.; Mallwitz, R.; "Highly Efficient Single-Phase Transformerless Inverters for Grid-Connected Photovoltaic Systems," *Industrial Electronics, IEEE Transactions on* , vol.57, no.9, pp.3118-3128, Sept. 2010.

[10] Shimizu, T.; Suzuki, S.; "A single-phase grid-connected inverter with power decoupling function," *Power Electronics Conference (IPEC), 2010 International*, vol., no., pp.2918-2923, 21-24 June 2010.

[11] Lai, J.-S.; Chen, D.; , "Design consideration for power factor correction boost converter operating at the boundary of continuous conduction mode and discontinuous conduction mode," Applied Power Electronics Conference and Exposition, 1993. APEC '93. Conference Proceedings 1993, Eighth Annual, vol., no., pp.267-273, 7-11 Mar 1993

[12] Rodriguez, C.; Amaratunga, G.A.J.; "Dynamic maximum power injection control of AC photovoltaic modules using current-mode control," Electric Power Applications, IEE Proceedings, vol.153, no.1, pp. 83- 87, 1 Jan. 2006

[13] "Fundamentals of Power Electronics (Second Edition)"; R. W. Erickson, D. Maksimovic.

[14] "100-W Universal Line Input PFC Boost Converter Using the UCC38050"; TI Application Note, Reference Design

[15] Lin Sun; Yongchun Liang; Chunying Gong; Yangguang Yan; , "Research on Single-Stage Flyback Inverter," Power Electronics Specialists Conference, 2005. PESC '05. IEEE 36th , vol., no., pp.849-854, 16-16 June 2005

[16] Youssef, E.B.; Stephane, P.; Bruno, E.; Corinne, A.; , "New P&O MPPT algorithm for FPGA implementation," IECON 2010 - 36th Annual Conference on IEEE Industrial Electronics Society , vol., no., pp.2868-2873, 7-10 Nov. 2010

[17] Zhigang Liang; Rong Guo; Huang, A.; , "A new cost-effective analog maximum power point tracker for PV systems," Energy Conversion Congress and Exposition (ECCE), 2010 IEEE , vol., no., pp.624-631, 12-16 Sept. 2010